

NATURAL OILS AS CORROSION INHIBITORS FOR STAINLESS STEEL IN SODIUM HYDROXIDE SOLUTIONS

M. Abdallah,^{1,2} I. Zaafarany, K. S. Khairou, and Y. Emad

We used electrochemical techniques (galvanostatic and potentiodynamic anodic polarization methods and also electrochemical impedance spectroscopy) to study corrosion inhibition by some natural oils (parsley, lettuce, sesame, arugula, and sweet almond oils) on the corrosion of type 304 stainless steel in 0.1 M NaOH solution. We show that the inhibition efficiency increases as the concentration of these oils increases. The inhibiting effect was attributed to adsorption of the major components of these oils on the stainless steel surface. The adsorption process is described by a Langmuir isotherm. It was found that incorporation of chloride ions in a 0.1 M NaOH solution accelerates pitting corrosion of the stainless steel as a result of shifting the pitting potential toward more negative values. Addition of the natural oils under study to sodium hydroxide solutions containing chloride ions shifts the pitting potential toward more positive values, indicating increased resistance of the steel to pitting corrosion. As the concentration of the oils under study in the solution increases, the charge transfer resistance increases while the capacitance of the double layer decreases.

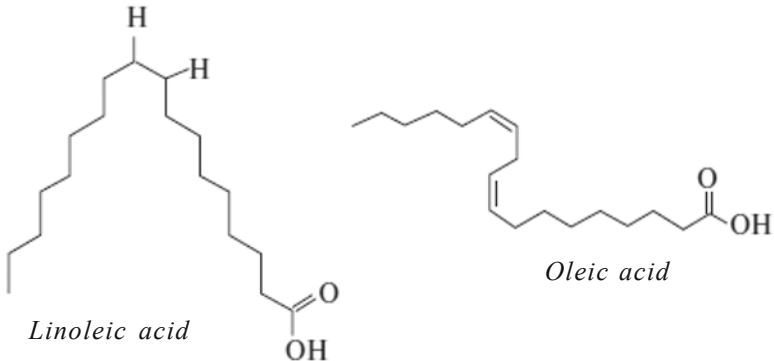
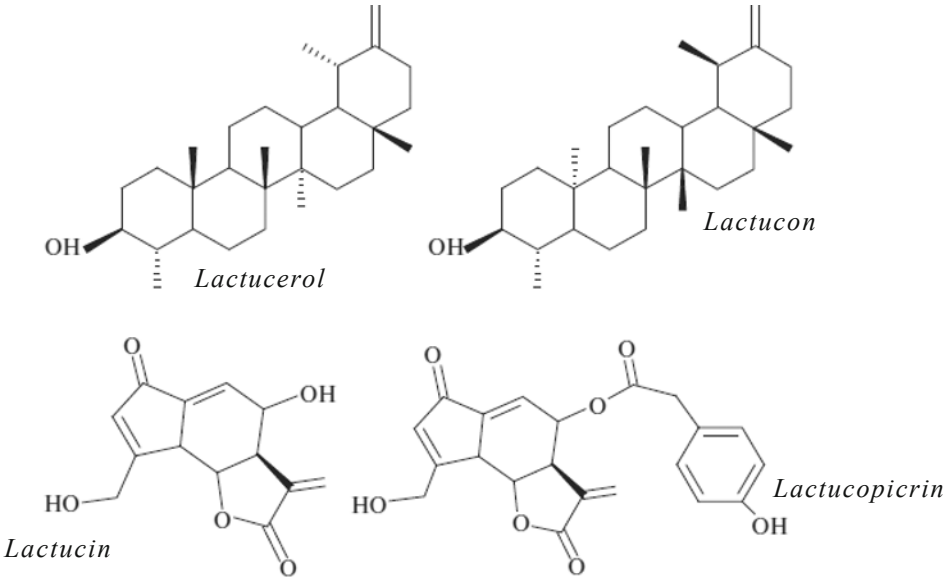
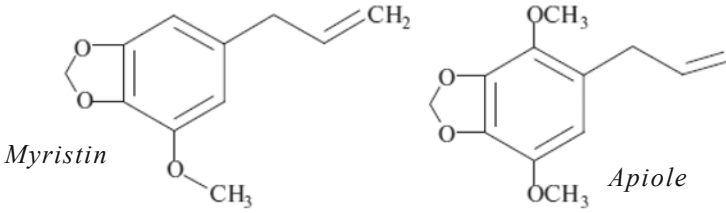
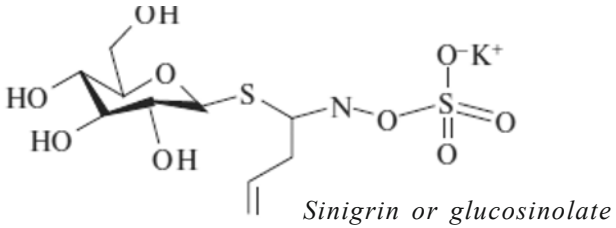
Key words: natural oils, 304 stainless steel, inhibitor, corrosion, adsorption.

Corrosion inhibitors are widely used to protect steel against corrosion: organic compounds containing nitrogen, oxygen, and sulfur atoms [1-6]. The efficiency of inhibitors depends on the characteristics of the metal surface and the presence of polar groups in the inhibitor molecules that act as adsorption centers on the metal surface. The environmental risk posed by many synthetic inhibitors has become the major reason for studying the feasibility of using natural oils as corrosion inhibitors. Natural oils are inexpensive, readily available, and environmentally friendly, and they are obtained from renewable resources [7]. Our previous papers [8-10] presented the results of investigation of some natural oils as corrosion inhibitors for metals and alloys [8-10]. The aim of this work is to study the inhibition efficiency of parsley, lettuce, sesame, arugula, and sweet almond oils relative to general and pitting corrosion of type 304 stainless steel in a 0.1 M sodium hydroxide solution.

¹ Chemistry Department, School of Applied Science, Umm Al-Qur University, Makkah Al Mukaramha, Saudi Arabia.

² Chemistry Department, School of Science, Benha University, Benha, Egypt. Translated from *Khimiya i Tekhnologiya Topliva i Masel*, No. 3, pp. 46 – 52, May – June, 2012.

Table 1

Oil	Structural formulas for major components
Sweet almond and sesame oils	 <p>The image shows two chemical structures. On the left is Linoleic acid, a long-chain polyunsaturated fatty acid with two double bonds. On the right is Oleic acid, a long-chain monounsaturated fatty acid with one double bond. Both are shown in their carboxylic acid form.</p> <p><i>Linoleic acid</i></p> <p><i>Oleic acid</i></p>
Lettuce	 <p>The image shows four chemical structures. The top two are Lactucic acid, a complex steroid-like molecule with multiple rings and functional groups. The bottom two are Lactucic acid, a complex molecule with a central ring system and various substituents.</p> <p><i>Lactucic acid</i></p> <p><i>Lactucic acid</i></p> <p><i>Lactucic acid</i></p> <p><i>Lactucic acid</i></p>
Parsley	 <p>The image shows two chemical structures. On the left is Myristin, a molecule with a benzene ring, a methoxy group, and a propenyl side chain. On the right is Apiole, a similar molecule with a methoxy group and a propenyl side chain.</p> <p><i>Myristin</i></p> <p><i>Apiole</i></p>
Arugula	 <p>The image shows the chemical structure of Sinigrin or glucosinolate, a complex molecule consisting of a glucose moiety linked to a sulfur atom, which is further linked to a nitrogen atom and a sulfonate group.</p> <p><i>Sinigrin or glucosinolate</i></p>

The stainless steel used in the experiments had the following chemical composition (wt.%): carbon, 0.07; manganese, 2; silicon, 1; phosphorus, 0.05; sulfur, 0.02; chromium, 19.5; nickel, 10.5; the remainder is iron. The electrode in the form of a cylindrical rod was secured to a pyrex glass tube using neutral wax, leaving 1 cm² exposed surface area. The electrode was first polished with different grades of emery paper to obtain a smooth surface, degreased with acetone, washed with twice-distilled water, and dried by rubbing between two filter papers. All the solutions were prepared using twice-distilled water. The electrochemical cell is described in [11].

Galvanostatic polarization was studied using a potentiostat with PS6 software to calculate the corrosion parameters. We used a cell with three compartments, containing a saturated calomel reference electrode (SCE) and an auxiliary electrode (platinum foil).

Potentiodynamic anodic polarization was studied at scanning rate 1 mV/s using a Wenking potentiostat (POS 73). A PL 3 x-y recorder was used to plot the current density vs. potential curves.

The percentage inhibition efficiency (*IE* in %) of the investigated oils against corrosion of the steel was calculated using the equation:

$$IE = \left(1 - I_{corr.add} / I_{corr.free}\right) 100$$

where $I_{corr.add}$ and $I_{corr.free}$ are the corrosion current densities in the presence of and in the absence of the inhibitor.

Electrochemical impedance spectroscopy was studied using a three-electrode glass cell similar to that used in studying the galvanostatic polarization. The experiments were carried out at 25±1°C at the open circuit potential over a frequency range of 1 kHz to 1 GHz, with a signal amplitude perturbation of 10 mV, using an IM6e system (Zahner Electric, Germany) and a personal computer. Nyquist plots were obtained from the measurement results. The charge transfer resistance R_{ct} was found from these plots by determining the difference in impedance at low and high frequencies, as shown in [12]. The double layer capacitance C_{dl} was calculated from the equation:

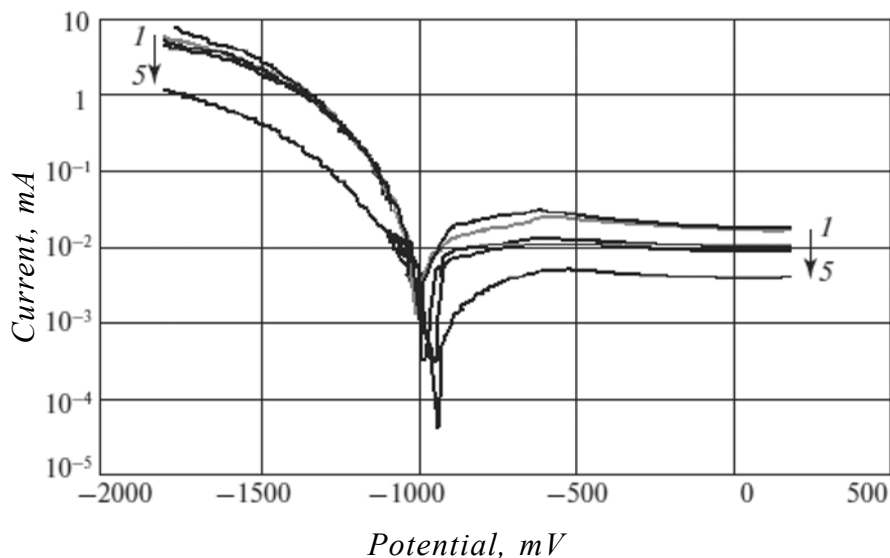


Fig. 1 Galvanostatic polarization curves for stainless steel in a 0.1 M sodium hydroxide solution containing sesame oil in a concentration of (ppm): 1 – 0; 2 – 200; 3 – 400; 4 – 600; 5 – 1000.

$$C_{dl} = \frac{1}{2\pi f_{max} R_{ct}}$$

where f_{max} is the frequency at which the imaginary part of the impedance Z_{imag} is maximum.

The inhibition efficiency and coverage of the steel surface by the oils were calculated from the equations:

$$IE = \left[\frac{(R_{ct} - R_{ct}^0)}{R_{ct}} \right] 100$$

$$\theta = \left[\frac{(R_{ct} - R_{ct}^0)}{R_{ct}} \right]$$

Table 2

Oil content in solution, ppm	$-b_a, mV/10$	$-b_c, mV/10$	$-E_{corr}, mV$	$I_{corr}, mA/cm^2$	θ	IE, %
No inhibitor						
0	124	135	1010	0.0780	-	-
Sweet almond oil						
200	337	145	1028	0.0050	0.9359	93.59
400	347	152	1038	0.0039	0.9500	95.00
600	350	160	1049	0.0031	0.9603	96.03
1000	353	171	1087	0.0029	0.9628	96.28
Lettuce oil						
200	226	268	1021	0.0092	0.8821	88.21
400	233	273	1032	0.0067	0.9141	91.41
600	235	383	1043	0.0046	0.9410	94.10
1000	242	408	1035	0.0013	0.9833	98.33
Parsley oil						
200	125	140	1016	0.0023	0.9705	97.05
400	138	148	1032	0.0017	0.9782	97.82
600	142	151	1049	0.0014	0.9821	98.21
1000	150	176	1071	0.0010	0.9872	98.72
Arugula oil						
200	169	115	1019	0.0099	0.8729	87.29
400	108	125	1031	0.0079	0.8987	89.87
600	167	132	1043	0.0048	0.9385	93.85
1000	180	145	1051	0.0046	0.9410	94.10
Sesame oil						
200	248	122	1014	0.0020	0.9744	97.44
400	268	134	1029	0.0019	0.9756	97.56
600	275	146	1047	0.0013	0.9828	98.28
1000	287	154	1080	0.0004	0.9949	99.49

where R_{ct}^0 and R_{ct} are the charge transfer resistances in the absence of and in the presence of the inhibitors.

The structural formulas of the major components of the studied oils are shown in Table 1 [13, 14].

Fig. 1 shows the galvanostatic polarization curves for stainless steel in a 0.1 M sodium hydroxide solution containing sesame oil in different concentrations. Similar curves were obtained for the other oils (not shown). We see that with an increase in the oil concentration, the rate of the anodic dissolution reaction decreases. In this case, the current vs. potential curves are shifted toward lower cathodic potential, while the cathodic Tafel lines are shifted toward higher cathodic potential.

The studied oils, like other adsorption inhibitors, are capable of selective adsorption, i.e., they are adsorbed on the inner portion of the electrical double layer. The adsorbed substances displace some of the H_3O^+ ions from the outer Helmholtz plane. This limits the accessibility of the metal surface for the reactive H_3O^+ ions. In other words, the oil blocks the steel surface and so the rate of the hydrogen evolution reaction decreases and consequently the rate of the overall corrosion reaction decreases.

Table 2 shows the effect of the natural oil concentration in solution on the corrosion current density I_{corr} , the cathodic Tafel slope b_c and the anodic Tafel slope b_a , the percentage inhibition efficiency, and the surface coverage on the steel. We see that as the oil concentration increases, the corrosion potential E_{corr} is shifted slightly toward more negative values, the corrosion current density decreases, and the percentage inhibition efficiency increases. This confirms that the studied oils have an inhibiting effect. The oils affect both the anodic and cathodic processes, i.e., they act as mixed inhibitors. The percentage inhibition efficiency decreases in the following order:

Sesame oil > lettuce oil > sweet almond oil > parsley oil > arugula oil.

The process of adsorption of the studied oils on the stainless steel surface can be described by an isotherm characterizing the steel surface coverage as a function of the oil concentration within the bulk of the solution at constant temperature. The surface coverage can be calculated from the equation:

$$\theta = 1 - \left(1 - I_{corr.add} / I_{corr.free} \right)$$

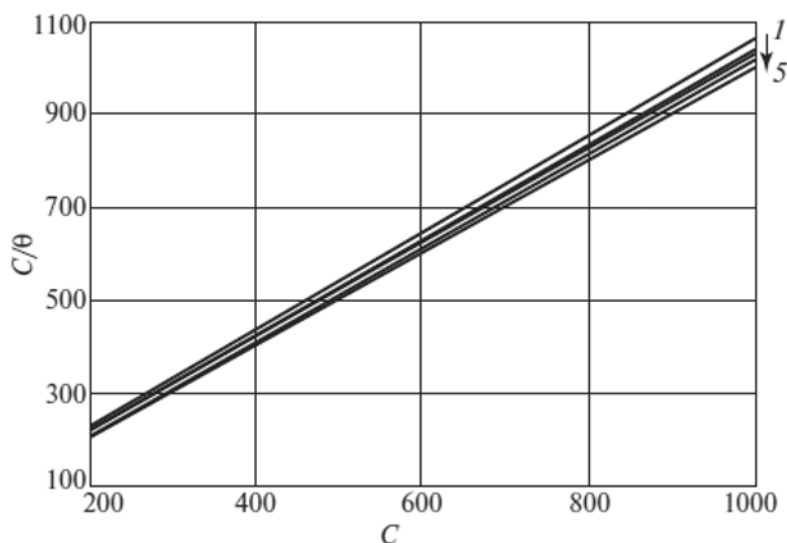


Fig. 2 Langmuir adsorption isotherms for: 1 – arugula oil; 2 – parsley oil; 3 – almond oil; 4 – lettuce oil; 5 – sesame oil.

Table 3

Oil	K	$-\Delta G_{ads}^D$, J/mol
Almond oil	0.128	4457.82
Lettuce oil	0.026	839.11
Parsley oil	0.194	5404.48
Arugula oil	0.043	1972.46
Sesame oil	0.117	4258.74

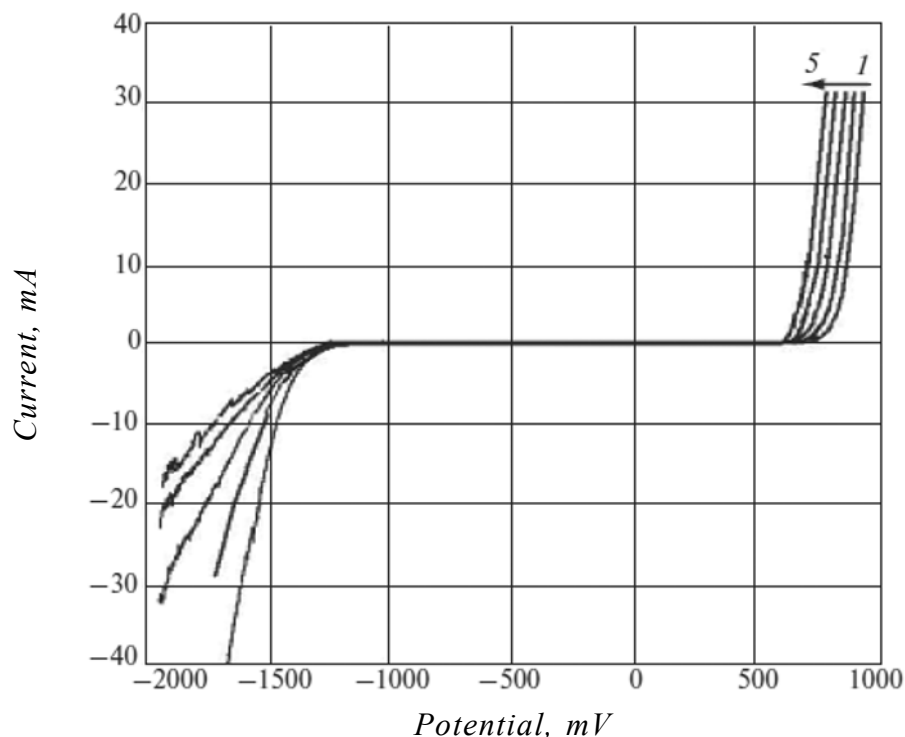


Fig. 3 Potentiodynamic anodic polarization curves for stainless steel in a 0.1 M sodium hydroxide solution for a sodium chloride concentration of (M): 1 - 0; 2 - 10^{-4} ; 3 - 10^{-3} ; 4 - 0.01; 5 - 0.1.

In order to choose the isotherm that best describes adsorption of the oils on the steel surface, we used the data in Table 2. We found that adsorption of the studied oils is described by a Langmuir isotherm:

$$C/\theta = 1/K + C$$

where K is the equilibrium constant for the adsorption process; C is the concentration of the inhibitor.

The plot of C/θ vs. C is a straight line (Fig. 2), which proves that the choice of a Langmuir isotherm is correct. From this we conclude that the adsorbed oil molecules do not interact with each other. The equilibrium constant for the adsorption process is related to the free energy of adsorption G_{ads}^0 [15, 16]:

$$K = (1/55.5)\exp(-\Delta G_{ads}^0 / RT)$$

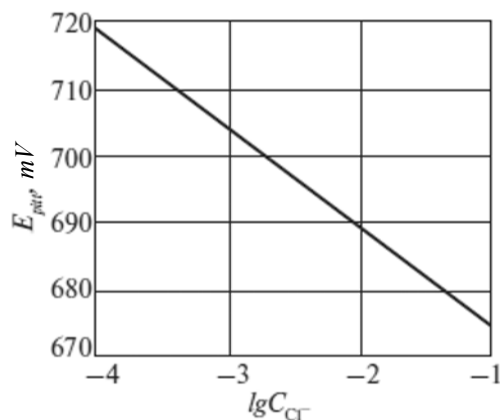


Fig. 4 Pitting potential of stainless steel vs. chloride ion concentration.

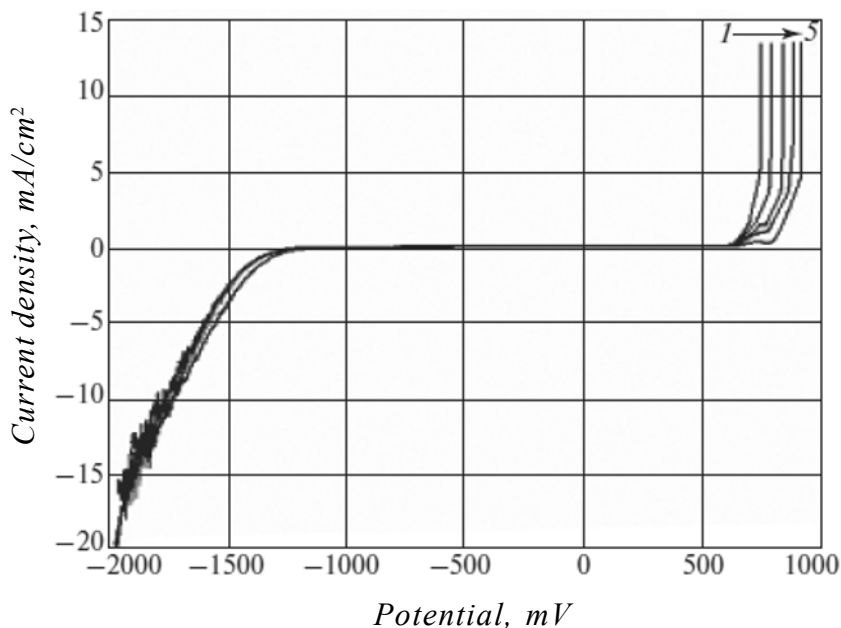


Fig. 5 Potentiodynamic anodic polarization curves for stainless steel in a solution containing 0.1 M sodium hydroxide and 0.1 M sodium chloride, for a sesame oil concentration in ppm: 1 – 0; 2 – 100; 3 – 400; 4 – 600; 5 – 1000.

where R is the universal gas constant; T is the absolute temperature; 55.5 is the concentration of water in the solution, mol/L.

The values of K and G_{ads}^0 calculated for the adsorption process on the stainless steel surface for all the oils are given in Table 3. The change in the free energy of adsorption is related to the water adsorption – desorption equilibrium, which makes a large contribution to the total free energy of adsorption. The negative values of G_{ads}^0 mean that adsorption of the studied oils on the steel surface is a spontaneous process.

We used potentiodynamic anodic polarization to study the effect of the sodium chloride concentration on pitting corrosion of stainless steel in a 0.1 M sodium hydroxide solution. **Fig. 3** shows the potentiodynamic anodic polarization curves for stainless steel electrodes, obtained for a scanning rate of 1 mV/s. We see that increasing the Cl^- ion content leads to a dramatic and sudden increase in corrosion current density at a certain potential, which indicates breakdown of the passivating film and initiation of corrosion pits. As the Cl^- ion

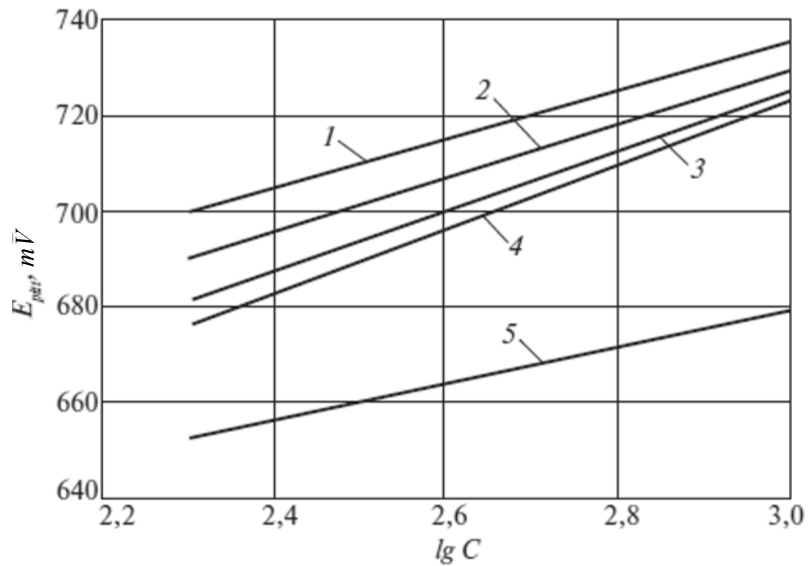


Fig. 6 Pitting potential of stainless steel vs. concentration of: 1 – sesame oil; 2 – lettuce oil; 3 – sweet almond oil; 4 – parsley oil; 5 – arugula oil.

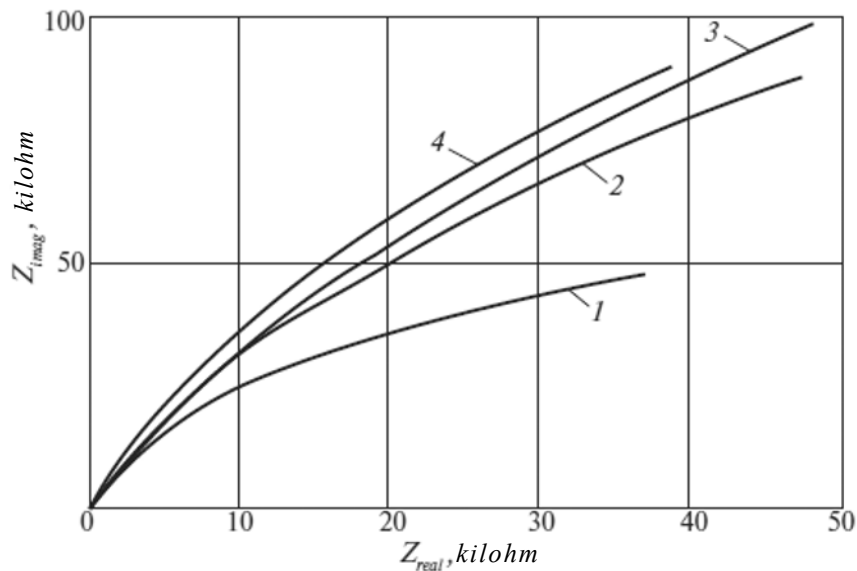


Fig. 7 Nyquist plot for stainless steel, for different sesame oil concentrations (ppm): 1 – 0; 2 – 200; 3 – 600; 4 – 1000.

concentration increases, the pitting potential is shifted toward more negative values. The breakdown of the passivating film can be explained by adsorption of chloride ions on the surface of this film, creating an electrostatic field between the film and the solution. When the electrostatic field strength reaches a certain value, the adsorbed anions begin to penetrate into the passivating film, initiating pitting corrosion. Pitting was visible on the surface of the electrodes after the experiments, where the number of pits per unit surface area increased as the concentration of Cl^- ions increased.

Fig. 4 shows the pitting potential E_{pitt} vs. the logarithm of the molar concentration C_{Cl} of the chloride ions. This dependence can be described by the equation:

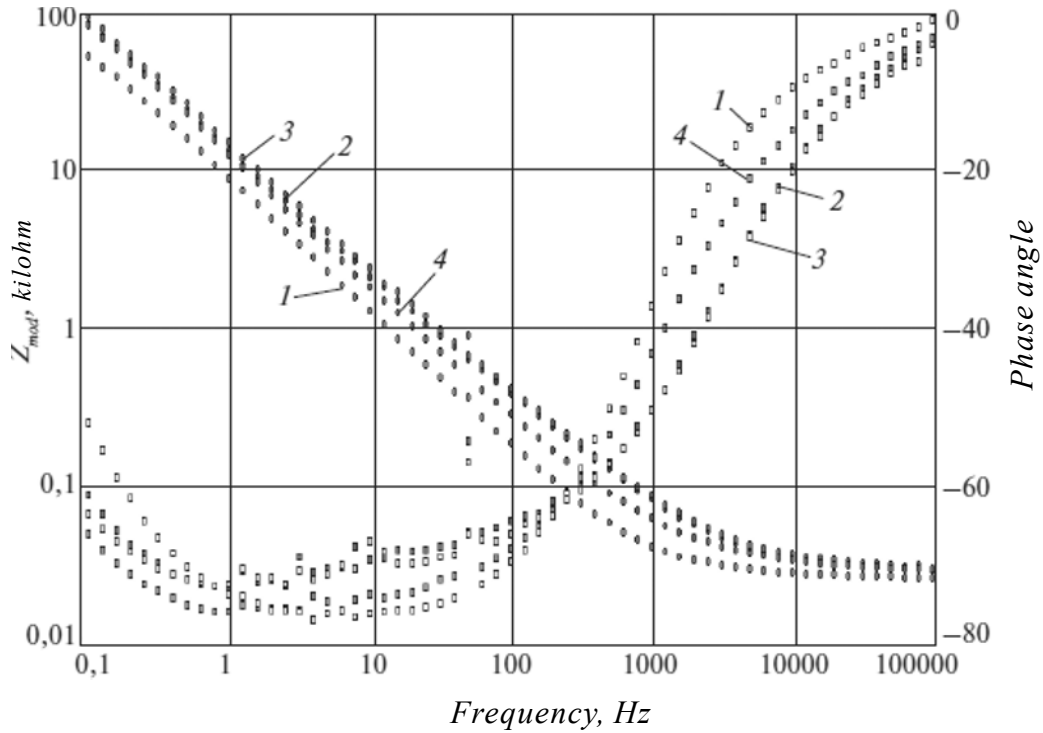


Fig. 8 Bode and phase angle plots for stainless steel, for different sesame oil concentrations (ppm): 1 – 0; 2 – 200; 3 – 600; 4 – 1000.

$$E_{pit} = a_1 + b_1 \log C_{Cl^-}$$

where a_1 and b_1 are constants depending on the nature of the electrode and the type of aggressive anion.

As already noted, as the concentration of chloride ions increases, the pitting potential is shifted toward more negative values, indicating breakdown of the passivating film and initiation of pitting corrosion.

Fig. 5 shows the potentiodynamic anodic polarization curves (scanning rate 1 mV/s) for stainless steel in a solution containing 0.1 M sodium hydroxide and 0.1 M sodium chloride with different concentrations of sesame oil. Similar curves were obtained for the other oils (not shown). We see that an increase in the oil concentration increases the pitting potential, which indicates increased resistance of the steel to pitting corrosion.

Fig. 6 shows the pitting corrosion potential for steel vs. the logarithm of the concentration (ppm) of the different oils. Increasing the oil concentration raises the pitting potential according to the equation:

$$E_{pit} = a_2 + b_2 \log C$$

where a_2 and b_2 are constants depending on the type of inhibitor, aggressive anion, and metal.

The inhibition efficiency decreases in the following order:

sesame oil > lettuce oil > sweet almond oil > parsley oil > arugula oil.

Electrochemical impedance spectroscopy lets us obtain detailed information about the process of protection of metal from corrosion using polymers, anodic films, and other coatings [17].

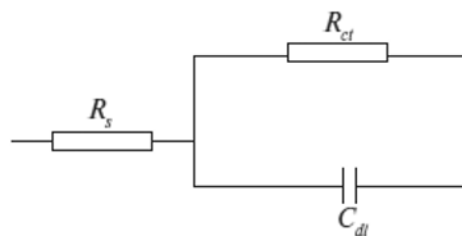


Fig. 9 Equivalent circuit.

Table 4

Oil concentration in solution, ppm	R_{ct} , kilohm	$C_{dl} \cdot 10^5, F$	$IE, \%$
<i>No inhibitor</i>			
0	113.3	2.329	–
<i>Almond oil</i>			
200	1484.0	2.174	92.36
600	1790.0	1.943	93.67
1000	1982.8	1.872	94.28
<i>Lettuce oil</i>			
200	1128.5	2.749	89.96
600	1254	2.176	90.96
1000	1364.8	2.938	91.69
<i>Parsley oil</i>			
200	944.8	3.597	88.00
600	1136.4	3.180	90.03
1000	1264.8	2.579	91.04
<i>Arugula oil</i>			
200	888.5	2.925	87.24
600	996.4	3.596	88.62
1000	1054.8	2.183	89.25
<i>Sesame oil</i>			
200	768.5	2.310	85.25
600	876.4	1.894	87.07
1000	984.8	1.955	88.49

We used electrochemical impedance spectroscopy at a temperature of 25°C to study the corrosion of stainless steel in a 0.1 M sodium hydroxide solution in the absence of and in the presence of the natural oils in different concentrations. Fig. 7 and Fig. 8 respectively show the Nyquist and Bode plots for steel in a 0.1 M sodium hydroxide solution in the presence of sesame oil. Similar curves were obtained for the rest of the oils (not shown). It was observed that the diameters of the circles corresponding to the curves increase with the oil concentration. This indicates that the polarization resistance of the oxide film increases with the oil concentration. The depressed capacitive curve is explained by surface roughness and inhomogeneity,

since this capacitive semicircle is connected with the dielectric properties and thickness of the protective oxide film [18]. We see that each total impedance diagram consists of a large capacitive loop with low frequency dispersion (inductive arc). The presence of this arc is explained by intermediates adsorbed on the anode, affecting the anodic process [19, 20]. For this reason, we disregarded the inductive arc. The impedance diagrams consisted of characteristic semicircles for all the solutions. This indicates that the steel dissolution process occurs under charge transfer control, and the presence of the inhibitors does not affect the mechanism of the steel dissolution process.

The impedance spectra were analyzed by approximating the data using a simple equivalent circuit model (Fig. 9). This circuit included a resistance R_s equivalent to the resistance of the solution, and a double layer capacitor of capacitance C_{dl} , placed in parallel to the charge transfer resistance R_{ct} . Table 4 gives the values of R_{ct} and C_{dl} for stainless steel in a 0.1 M sodium hydroxide solution containing the oil in different concentrations.

The impedance diagram obtained shows that corrosion of steel is mainly controlled by a charge transfer process. Analyzing the data in Table 4, we should point out that R_{ct} increases with the inhibitor concentration, meaning an increase in the inhibition efficiency. The capacitance of the double layer decreases with an increase in the inhibitor concentration, which is due to adsorption of components of the oils on the electrode surface, leading to formation of a protective film. The inhibition efficiency decreases in the order:

sesame oil > lettuce oil > sweet almond oil > parsley oil > arugula oil.

From the results of our research, it is obvious that the efficiency of the oils as corrosion inhibitors depends on the nature of the oil and its concentration. With an increase in the oil concentration in solution, we observe the following:

- a decrease in the corrosion current density;
- an increase in inhibition efficiency;
- an increase in the surface coverage;
- a shift in the pitting potential toward more positive values;
- an increase in the charge transfer resistance.

The results of our observations indicate that corrosion inhibition is due to adsorption of oils at the solution/metal interface. The nature of the interaction of the inhibitor with the metal surface can be explained from the standpoint of the adsorption parameters [21, 22]. The inhibition process depends on many factors [23]: the number of active centers in the inhibitor molecule, the charge density, the molecular size and structure, and the mode of interaction with the metal surface and ability to form a complex with it [24, 25]. Based on the structural formulas of the major components of the studied oils, we assume that formation of a complex between the oil molecules and the metal surface is impossible. This means that inhibition occurs due to adsorption of inhibitor molecules on the steel surface. The adsorption layer plays the role of a barrier between the metal surface and the aggressive solution.

Calculations by different methods give the same order of the inhibitors with respect to inhibition efficiency, indicating that the experimental data are consistent. Any discrepancy between the inhibition efficiencies obtained by different methods is due to the different experimental conditions.

REFERENCES

1. Xian Ghong Li, Schuduan Dang, and Hui Fu, "Three pyrazine derivatives as corrosion inhibitors for steel in 1.0 M H_2SO_4 solution," *Corros. Sci.*, **53**, 3241 (2011).
2. M. Abdallah, "Behavior of 304 stainless steel in sulphuric acid solution and its inhibition by some substituted pyrazolones," *Mater. Chem. and Phys.*, **82**, 768 (2003).

3. A. S. Fouda, M. Abdallah, S. M. Al-Ashrey, and A. A. Abdel-Fattah, "Some crown ethers as inhibitors for corrosion of stainless steel 304 in aqueous solution," *Desalination*, **250**, 538 (2010).
4. A. S. Fouda, "Inhibition effect of phenylthiazole derivatives on corrosion of 304 L stainless steel in HCl solution," *Corros. Sci.*, **51**, 868 (2009).
5. X. L. Cheng, H. Y. Ma, S. H. Chen, R. Yu, X. Chen, and Z. M. Yao, "Corrosion of stainless steels in acid solutions with sulfur-containing compounds," *Corros. Sci.*, **41**, 321 (1999).
6. S. A. Abd El-Maksoud and A. S. Fouda, "Some pyridine derivatives as corrosion inhibitors for carbon steel in acidic medium," *Mater. Chem and Phys.*, **93**, 84 (2005).
7. A. Singh, I. Ahamad, V. K. Singh, and M. A. Quraishi, "Inhibition effect of environmentally benign karanj (*Pongamia Pinnata*) seed extract on corrosion of mild steel in hydrochloric acid solution," *J. Solid State Electrochem.*, **15**, 1087 (2011).
8. M. Abdallah, S. O. Al-Karane, and A. A. Abdel-Fattah, "Inhibition of acidic and pitting corrosion of nickel using natural black cumin oil," *Chem. Eng. Comm.*, **197**, 1446 (2010).
9. M. Abdallah, S. O. Al-Karane, and A. A. Abdel-Fattah, "Inhibition of corrosion of nickel and its alloys by natural clove oil," *Chem. Eng. Comm.*, **196**, 1406 (2009).
10. M. Abdallah, M. A. Radwan, S. M. Shohayeb, and S. Abdelhamed, "Use of some natural oils as crude pipeline corrosion inhibitors in sodium hydroxide solutions," *Chemistry and Technology of Fuels and Oils*, **46**, No. 5, 354 (2010).
11. A. Y. El-Etre, "Inhibition of acid corrosion of carbon steel using aqueous extract of olive leaves," *J. Colloid Interface Sci.*, **314**, 578 (2007).
12. T. Tsuru, S. Haruyama, and G. Boshoku, "Basics of corrosion measurements," *J. Japan Soc. Corros. Eng.*, **27**, 573 (1978).
13. E. B. Truitt, G. Duritz, and E. M. Ebersberger, "Evidence of monoamine oxidase inhibition by myristicin and nutmeg," *Proc. Soc. Exp. Biol. Med.*, **112**, 647 (1963).
14. Richard D. Hubant, *J. Agric. Food Chem.*, **54**, No. 7, 2678 (2006).
15. M. Kliskic, J. Radosevic, and S. Gndic, *J. Appl. Electrochem.*, **27**, 947 (1994).
16. M. Abdallah, "Tetradecyl-1,2-diol propenoxyates as inhibitors for corrosion of aluminum in hydrochloric acid," *Bull. Electrochem.*, **16**, No. 6, 258 (2000).
17. T. P. Hoar and G. G. Wood, *J. Electrochim. Acta*, **7**, 333 (1964).
18. M. Metikos-Hukovic, R. Bobic, Z. Gwabac, and S. Brinic, *J. Appl. Electrochem.*, **24**, 772 (1994).
19. A. Caprani, I. Epelboin, Ph. Morel, and H. Takenouti, in: *Proceedings of the Fourth European Symposium On Corrosion Inhibitors, Ferrara, Italy* (1975), p. 571.
20. I. Epelboin, M. Keddou, and H. Takenouti, *J. Appl. Electrochem.*, **2**, 71 (1972).
21. I. Sekine, M. Sabongi, H. Hagiuda, T. Oshibe, M. Yuasa, T. Imahc, Y. Shibata, and T. Wake, *J. Electrochem. Soc.*, **139**, 3167 (1992).
22. X. Li, S. Deng, H. Fen, and T. Li, *Electrochim. Acta*, **54**, 4089 (2009).
23. A. S. Fouda, M. Mousa, F. Taha, and A. I. Eleanaa, *J. Corros. Sci.*, **26**, 719 (1986).
24. M. Abdallah, "Antibacterial drugs as corrosion inhibitors of corrosion of aluminum in hydrochloric acid solution," *Corros. Sci.*, **46**, 1981 (2004).
25. F. M. Al-Nowaiser, M. Abdallah, and E. H. El-Mossalamy. E. H., "Rosemary oil as a corrosion inhibitor of carbon steel in 0.5 M sulfuric acid solution," *Chemistry and Technology of Fuels and Oil*, **47**, No. 1, 66 (2011).